

Open-Circuit Voltage, Fill Factor, and Efficiency of a CdS/CdTe Solar Cell

L. A. Kosyachenko[^] and E. V. Grushko

Yuriy Fedkovych Chernivtsi National University, ul. Kotsubinskyi 2, Chernivtsi, 58012 Ukraine

[^]e-mail: lakos@chv.ukrpack.net

Submitted April 19, 2010; accepted for publication April 26, 2010

Abstract—The dependences of the open-circuit voltage, fill factor, and efficiency of the thin-film CdS/CdTe solar cell on the resistivity ρ and carrier lifetime τ in the absorbing CdTe layer were studied. In the common case in which the uncompensated acceptor concentration and the electron lifetime in the CdTe layer are within 10^{15} – 10^{16} cm⁻³ and 10^{-10} – 10^{-9} s, the calculation results correspond to the achieved efficiency of the best thin-film CdS/CdTe solar cells. It was shown that, by decreasing ρ and increasing τ in the absorbing CdTe layer, the open-circuit voltage, fill factor, and efficiency can be substantially increased, with their values approaching the theoretical limit for such devices.

DOI: 10.1134/S1063782610100234

1. INTRODUCTION

Within the last 10–15 years, the CdS/CdTe heterostructure has been considered the most promising for semiconductor solar power engineering [1–3]. The attained efficiency of laboratory samples of thin-film CdS/CdTe solar cells on glass substrates with transparent ITO or/and SnO₂ coating is 16.5% [4–7]; for larger-area (more than 0.5 m²) modules, it is ~10% [8, 9]. Despite the long-term efforts of scientists and technologists, even the record efficiency of solar cells of this type ranks below the theoretical limit of 28–30% [10]. One of the causes of such a state of the art is probably the fact that the effect of all the main parameters of used materials and the CdS/CdTe diode structure itself on photoelectric conversion has not been considered comprehensively in most published papers.

In [11], the dependences of the short-circuit current density J_{sc} of the CdS/CdTe solar cell on the absorbing CdTe layer parameters were analyzed in their combination (layer thicknesses, uncompensated acceptor concentration, electron lifetime, and surface recombination velocity) were analyzed. Taking into account the loss for recombination at the CdTe–CdS interface on the CdTe layer rear surface and in the space-charge region (SCR), the conditions were found, under which photogenerated charge collection comes close to be complete. However, if we use parameters of actual thin-film CdS/CdTe solar cells, the calculation results are close to experimentally observed J_{sc} .

In this paper, we analyze the effect of the parameters of the diode structure on other key photoelectric characteristics of the CdS/CdTe solar cell, such as the open-circuit voltage; the fill factor of the current–voltage (I – V) characteristic during irradiation; and, taking into account the consideration of the charge

collection efficiency in [11], the device efficiency. This analysis is preceded by the validation of the charge transport mechanism, the depletion layer width in the thin-film CdS/CdTe heterostructure, and its energy-level diagram, which is required for further calculations.

2. CURRENT–VOLTAGE CHARACTERISTIC OF THE CdS/CdTe HETEROSTRUCTURE

The determination of the open-circuit voltage and solar cell efficiency implies knowledge of its I – V characteristic, the general form of which can be written as

$$J(V) = J_d(V) - J_{ph}, \quad (1)$$

where $J_d(V)$ is the current density in the absence of irradiation (dark current) and J_{ph} is the density of the current excited by incident radiation, i.e., the photocurrent density. For the so-called “ideal” solar cell, the dark current is described by the Shockley equation

$$J_d(V) = J_s \left[\exp\left(\frac{qV}{kT}\right) - 1 \right], \quad (2)$$

where J_s is the saturation current density equal to the reverse current through the diode and independent of voltage at $qV \gg kT$ (q is the elementary charge, k is the Boltzmann constant, and T is the temperature).

The actual I – V characteristic of the CdS/CdTe solar cell differs from that described by formula (2). In many cases, the forward current can be described by an expression similar to (2), introducing the exponent qV/nkT (instead of qV/kT), where n is the so-called “ideality” coefficient, which is typically (but not always) equal to 1–2. To a certain extent, the theory

can be made consistent with experiment by adding the recombination component $J_0[\exp(qV/2kT) - 1]$, where J_0 is a new quantity independent of V , to the dark current in Eq. (1). However, our studies show that such generalizations of formulas (1) and (2) do not cover the observed variety of CdS/CdTe heterostructure characteristics. In the actual case, the voltage dependence of the forward current is not always exponential and reverse current saturation is never observed (the latter has not been remarked in publications at all). At the same time, the experimental characteristics of the CdS/CdTe heterostructure and their temperature evolution are very well described by the Sah–Noyce–Shockley generation–recombination theory [12].

According to this theory, the dependence $U \propto \exp(qV/nkT)$ at $n \approx 2$ takes place only when the generation–recombination level is near the midgap. However, if this level is far from the midgap, the coefficient n becomes close to unity, but only at low biases. As the voltage is increased, the $I-V$ characteristic transforms into the dependence with $n \approx 2$; at even larger voltages, the dependence of I on V becomes weaker [12, 13]. At large forward currents, the voltage drop at the series resistance R_s of the bulk region of the CdTe layer should also be taken into account by replacing the voltage V in the obtained formulas by the sum $V + IR_s$. The reverse portion of the characteristic is also well described within the Sah–Noyce–Shockley models.

According to the Sah–Noyce–Shockley theory, the generation–recombination rate is given by [12]

$$U(x, V) = \frac{n(x, V)p(x, V) - n_i^2}{\tau_{p_0}[n(x, V) + n_1] + \tau_{n_0}[p(x, V) + p_1]}, \quad (3)$$

where $n(x, V)$ and $p(x, V)$ are the carrier concentrations in the conduction and valence bands, n_0 and p_0 are their equilibrium values, and τ_{n_0} and τ_{p_0} are the effective lifetimes of electrons and holes in the depletion layer, respectively. The quantities n_1 and p_1 are defined by the energy distance E_t of the recombination level from the valence band top, i.e., $p_1 = N_v \exp(-E_t/kT)$ and $n_1 = N_c \exp[-(E_t - E_g)/kT]$, where $N_c = 2(m_n kT/2\pi\hbar^2)^{3/2}$ and $N_v = 2(m_p kT/2\pi\hbar^2)^{3/2}$ are the effective densities of states in the conduction and valence bands and m_n and m_p are electron and hole effective masses, respectively.

The recombination (under forward bias) and generation (under reverse bias) current densities are found by integrating $U(x, T)$ over the entire depletion layer,

$$J_{gr} = q \int_0^W U(x, V) dx, \quad (4)$$

in the chosen reference frame, the expressions for the electron and hole concentrations $n(x, V)$ and $p(x, V)$ are given by [13]

$$p(x, V) = N_c \exp\left[-\frac{\Delta\mu + \phi(x, V)}{kT}\right], \quad (5)$$

$$p(x, V) = N_v \exp\left[-\frac{E_g - \Delta\mu - \phi(x, V) - qV}{kT}\right], \quad (6)$$

where $\Delta\mu$ is the energy distance of the Fermi level from the valence band top in the neutral CdTe layer region and $\phi(x, V)$ is the hole potential energy in the depletion layer (see Section 3).

3. SPACE-CHARGE REGION WIDTH IN THE THIN-FILM CdS/CdTe HETEROSTRUCTURE

One of the most important parameter of the solar cell, which essentially controls its electrical and photoelectric characteristics, is the SCR width W appearing in Eq. (4). It is supposed that the n -CdS layer ($n = 10^{16}-10^{17} \text{ cm}^{-3}$) in the effective CdS/CdTe solar cell is not involved in photoelectric conversion, but serves only as a “window” through which radiation is fed to the absorbing layer, introducing certain losses due to absorption in the spectral region $\lambda < 500-520 \text{ nm}$. In discussing the energy diagram of the thin-film CdS/CdTe solar cell, the energy band bending in CdS near the CdS–CdTe interface is shown as hardly discernible or is not shown at all (see, e.g., [2, 14, 15]). Nevertheless, when analyzing the conditions of high efficiency of the CdS/CdTe heterostructure, we have to assume the uncompensated acceptor concentration in the CdTe layer to be $10^{16}-10^{17} \text{ cm}^{-3}$ and even higher. It may seem that the depletion layers in CdS and CdTe appear comparable in width in this case and the commonly used model of the sharply asymmetric $p-n$ heterojunction becomes unacceptable. Doubts are resolved if we take into account that the electron concentration in the conduction band n controlling the CdS layer resistivity and the uncompensated donor concentration $N_d - N_a$ controlling the SCR width in this layer are identical only if the material conductivity is controlled by a donor forming a shallow level with an ionization energy lower than the thermal energy kT (when it can be assumed that impurity atoms are fully ionized).

In fact, the CdS layer contains a significant number of donor and acceptor impurities (defects) which introduce both shallow and deep energy levels into the band gap. The self-compensation effect [16] is inherent to this material, as well as to other II–VI compounds, i.e., CdS is always a semiconductor compensated to a greater or lesser extent. In this case, as is known, the Fermi level is “pinned” (pinning effect) by the level with the degree of compensation N_a/N_d of which does not too much differ from 1/2 (if the level is

sufficiently deep, the Fermi level is identical to it at $N_a/N_d = 1/2$) [7]. As follows from the statistics of electrons and holes in the compensated semiconductor, the value of $N_d - N_a$ in CdS can differ significantly from the electron concentration n in the conduction band. For example, if the ionization energy and donor impurity concentration are sufficiently high and the compensating acceptor impurity concentration is two times lower, the Fermi level will obviously coincide with the acceptor level in a wide temperature range. In this case, the electron concentration in the conduction band and, hence, the material resistivity at an unchanged degree of compensation can vary by many orders of magnitude, depending on the ionization energy of the compensated impurity. Thus, the uncompensated donor concentration $N_d - N_a$ in the CdS layer can significantly exceed the electron concentration n in the conduction band; hence, equating $N_d - N_a$ and n , we can make a serious error. Due to a significant content of impurities and defects, the uncompensated donor concentration in the CdS layer may be much higher than the electron concentration in the conduction band and the CdS/CdTe depletion layer of the diode structure is almost completely concentrated in CdTe even in the case of a rather high-resistivity CdS layer (Fig. 1) [2, 14, 15]. The potential energy $\varphi(x, V)$ behavior and the expression for the depletion layer width in the n -CdS/ p -CdTe heterostructure can be written, as for the Schottky diode or for a sharply asymmetric $p-n$ junction, in the form [10]

$$\varphi(x, V) = (\varphi_0 - qV) \left(1 - \frac{x}{W}\right)^2, \quad (7)$$

$$W = \sqrt{\frac{\varepsilon \varepsilon_0 (\varphi_0 - qV)}{q^2 (N_a - N_d)}}, \quad (8)$$

where ε is the relative permittivity of the semiconductor, ε_0 is the permittivity of free space, φ_0 is the barrier height in equilibrium with the semiconductor ($\varphi_0 = aV_{bi}$, where V_{bi} is the diffusion potential), and $N_a - N_d$ is the uncompensated acceptor concentration in the CdTe layer.

4. MINORITY CARRIER CURRENT IN THE CdS/CdTe HETEROSTRUCTURE

Above-barrier carrier flow in the heterostructure under study is limited by rather high barriers for both holes and electrons (Fig. 1). Indeed, in equilibrium ($V = 0$), the barrier height for the hole flow from CdTe to CdS is $E_g_{\text{CdS}} - \Delta\mu_{\text{CdS}} - \Delta\mu$, where $\Delta\mu_{\text{CdS}}$, as before, is the distance from the Fermi level to the conduction band bottom in CdS; $\Delta\mu$ is the distance from the Fermi level to the valence band in the CdTe layer bulk, equal to $kT \ln(N_v/p)$; and p is the hole concentration, which depends on the CdTe resistivity. The energy barrier preventing electron flow from CdS to CdTe is appre-

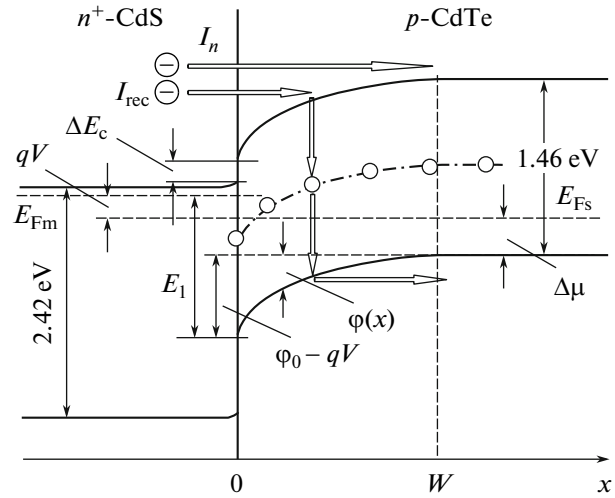


Fig. 1. Energy diagram of the CdS/CdTe heterojunction under forward bias. The electronic transition corresponding to the recombination I_{rec} and above-barrier I_n currents are shown.

ciably lower, but is also rather high; at $V = 0$, it is $E_g - \Delta\mu$ (E_g is the CdTe bandgap).

Therefore, at low forward biases, the dominant mechanism of charge transport is recombination in the depletion layer (the current I_{rec} in Fig. 1). However, as qV approaches φ_0 , the above-barrier current eventually becomes comparable to the recombination current and then exceeds it due to a sharper voltage dependence.

Since the barrier for holes in the CdS/CdTe heterostructure is much higher than that for electrons, the electron component dominates in the above-barrier current. It is clear that the electron current flow is similar to that in the $p-n$ junction, and the density of the above-barrier (diffusion) electron current can be written as [10]

$$J_n = q \frac{n_p L_n}{\tau_n} \left[\exp\left(\frac{qV}{kT}\right) - 1 \right], \quad (9)$$

where n_p is the electron density in the p -layer bulk, given by $N_c \exp[-(E_g - \Delta\mu)/kT]$; τ_n is the electron lifetime; $L_n = \sqrt{\tau_n D_n}$ is the electron diffusion length; and D_n is the diffusion coefficient of electrons related to their mobility μ_n by the Einstein relation $qD_n/kT = \mu_n$.

5. COMPARISON WITH EXPERIMENTAL DATA

Glass plates with a semitransparent $\text{SnO}_2 + \text{In}_2\text{O}_3$ (ITO) conductive layer were used as substrates for the solar cells under study. A CdS layer 0.1 μm thick and CdTe layer 4–5 μm thick were grown by chemical bath deposition and close-space sublimation, respectively. The ohmic contact with CdTe was formed by Ni thermal evaporation in vacuum (10^{-6} Torr) at a substrate

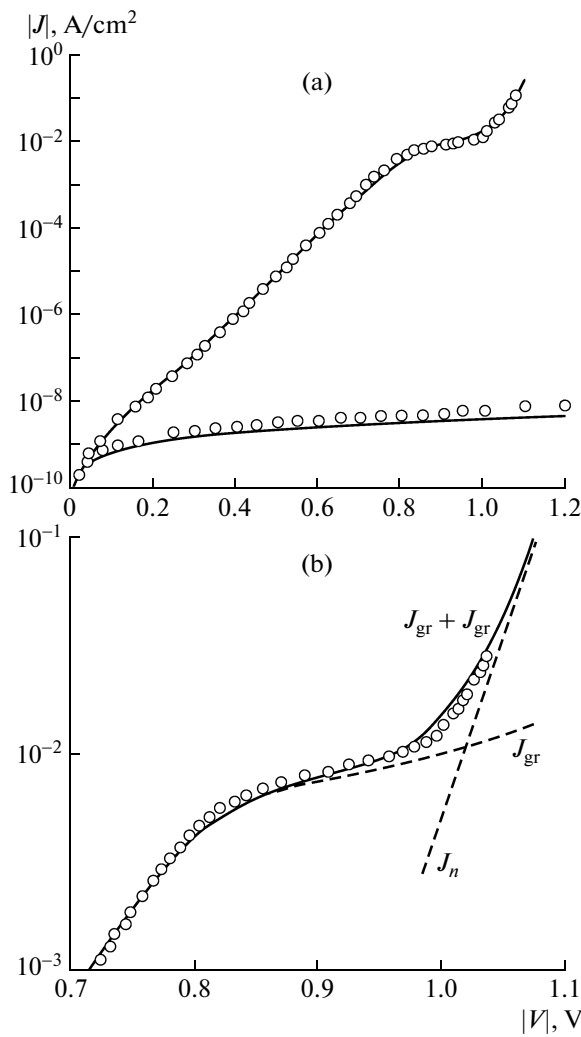


Fig. 2. (a) Current–voltage characteristic of the studied CdS/CdTe thin-film solar cell. Circles are experimental data, and solid curves are the results of calculations by formula (10), taking into account (4)–(9). (b) Comparison of the calculated and experimental dependences in the region of high forward currents (J_{gr} and J_n are the recombination and above-barrier components, respectively).

temperature of 150–200°C after preliminary CdTe surface treatment with ~500-eV argon ions. Under conditions of solar irradiation (standard AM1.5 solar spectrum), the short circuit-current density was close to 18 mA/cm², the open-circuit voltage was ~0.85 V, and the efficiency was about 7%.¹

Figure 2 shows the I – V characteristic reflecting the general features of the thin-film CdS/CdTe heterostructure. The forward portion contains an extended region (within six orders of magnitude), where the dependence $I \propto \exp(qV/nkT)$ is valid at $n = 1.92$. In the region of high current densities $J > 1 \text{ mA/cm}^2$, a

¹ Our objective was to determine the causes of the observed relatively low photoelectric efficiency of the CdS/CdTe heterostructure, rather than to demonstrate a highly efficient solar cell.

deviation from the exponential dependence is observed, which (it should be emphasized) is caused by features of recombination processes in the SCR, rather than by the voltage drop across the resistance R_s of the neutral region of the CdTe layer [18, 19]. As the voltage further increases (>1 V), a sharper current increase is observed.

The reverse current exhibits a sublinear voltage dependence at the relatively low level $J = 10^{-9}$ – 10^{-8} A/cm^2 , which indicates a fairly high quality of the CdS/CdTe heterostructure and the absence of its perceptible shunting. According to the above consideration, the dark current density in the CdS/CdTe heterostructure (expression (1)) should be presented by the sum of the generation–recombination and above-barrier components defined by expressions (4) and (9),

$$J_d(V) = J_{gr}(V) + J_n(V). \quad (10)$$

Figures 2a and 2b compare the experimental I – V characteristic (circles) with the I – V characteristic calculated according to the above-stated theory (solid curves). In calculating the carrier lifetimes $\tau_{n0} = \tau_{p0} = \tau$ in the SCR were set equal to $1.2 \times 10^{-10} \text{ s}$ (the value of τ defines the current magnitude, but has no effect on the curve shape), the resistivity was $\rho = 0.05 \Omega \text{ cm}$ (it yields $\Delta\mu = 0.031 \text{ eV}$), the ionization energy of the generation–recombination center was $E_t = 0.73 \text{ eV}$ (E_t defines the rectification factor), and the barrier height φ_0 and the uncompensated acceptor concentration $N_a - N_d$ were taken as 1.13 eV and 10^{17} cm^{-3} , respectively. We can see that the characteristic calculated by formula (10) taking into account (4)–(9) is in very good agreement with the results of measurements of both the forward and reverse currents.

The Sah–Noyce–Shockley theory describes the entire variety of the experimentally observed characteristics of the CdS/CdTe heterostructure. As an example, Fig. 3 shows the forward characteristics calculated at various parameters of the CdTe layer.

The carrier lifetime in the calculation was taken as 10^{-11} and 10^{-8} s , which seems to be characteristic of not too perfect and rather perfect CdTe layers. We can see that the forward current exponentially increases with voltage within more than six orders of magnitude in the case of $\tau = 10^{-11} \text{ s}$ when the recombinative mechanism of charge transport dominates. As the material resistivity ρ decreases from 10^3 to $10^{-1} \Omega \text{ cm}$, the “ideality” factor n appearing in the commonly used semi-empirical formula decreases from 1.92 to 1.74. In the case of $\tau = 10^{-9} \text{ s}$, the recombination current dominates only at voltages lower than 0.5–0.6 V and $\rho = 10^{-1}$ – $10^3 \Omega \text{ cm}$ ($n = 1.8$ –1.9).

At low resistivities $\rho = 10^{-1}$ – $10 \Omega \text{ cm}$, the current in the voltage region where the recombinative mechanism of charge transport dominates obeys the dependence $I \propto \exp(qV/nkT)$ at $n \approx 1.9$ within about nine orders of magnitude. However, at current densities higher than 0.1 mA/cm^2 , the exponential dependence $I(V)$ is violated and features similar to those shown in

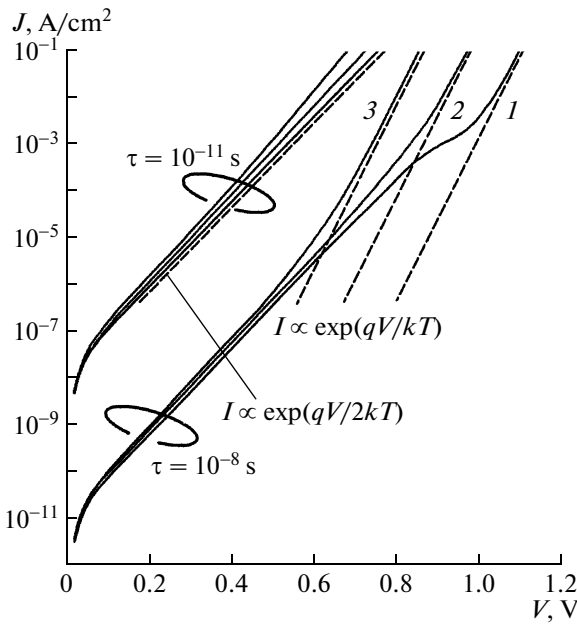


Fig. 3. Forward current–voltage characteristic of the CdS/CdTe heterostructure, calculated at carrier lifetimes of 10^{-8} and 10^{-11} s and CdTe layer resistivities of (1) 0.1, (2) 10, and (3) $10^3 \Omega \text{ cm}$ (the hole concentrations are 10^{18} , 10^{16} , and 10^{14} cm^{-3} , respectively).

Fig. 2 are observed. It should be emphasized that such features are within the current range of most practical interest, since the short-circuit current density of the CdS/CdTe solar cell should exceed at least 15–20 mA/cm².

If the CdTe layer resistivity is 10^2 – $10^3 \Omega \text{ cm}$, above-barrier electron transport dominates at current densities of 15–20 mA/cm², since ϕ_0 decreases due to increasing $\Delta\mu$. Thus, the assumption of the crucial role of the recombination current, proceeding from a simplified model that ignores the above features of the I – V characteristic, can lead to significant errors when analyzing the material parameters providing maximum possible open-circuit voltages and fill factors [20, 21].

6. RESULTS OF CALCULATIONS OF THE OPEN-CIRCUIT VOLTAGE, FILL FACTOR, AND EFFICIENCY

Let us consider the efficiency of photoelectric conversion of radiation, ignoring optical losses due to reflections from interfaces and absorption in the transparent layer and CdS film.

To determine the open-circuit voltage V_{oc} and the fill factor of the CdS/CdTe solar cell, we should know the short-circuit current J_{sc} , that is represented by the sum of two components: (i) the photocurrent caused by photogeneration of electron–hole pairs in the SCR and (ii) the neutral region of the p -CdTe layer (the *drift*

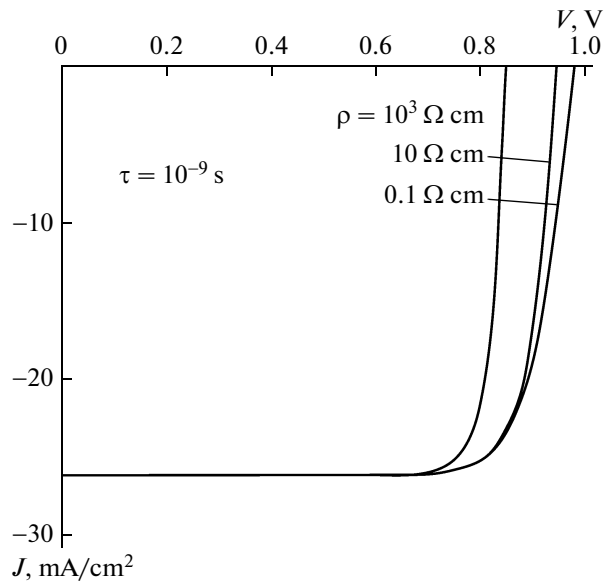


Fig. 4. Current–voltage characteristic of the CdS/CdTe heterostructure under conditions of AM1.5 solar irradiation ($J_{sc} = 26 \text{ mA/cm}^2$), calculated at the carrier lifetime of 10^{-9} s and various resistivities of the absorbing p -CdTe layer.

and diffusion J_{sc} components, respectively). It may seem that it would be desirable for better charge collection if the entire radiation were to be absorbed in the SCR, for which its width W should be larger than the radiation penetration depth in the CdTe layer. In fact, this is not always the case, since SCR expansion results in a decrease in the electric field strength, which leads to an increase in the recombination rate at the CdTe–CdS interface; simultaneously, the photocurrent diffusion component decreases. Therefore, the charge collection efficiency increases only to a certain extent as a narrow SCR expands. In practical CdS/CdTe solar cells, the minority carrier lifetime τ_n is within 10^{-10} – 10^{-9} s [21]. As shown in [11], at such τ_n , maximum J_{sc} is 26–27 mA/cm², but only if the uncompensated acceptor concentration in the CdTe layer is within 10^{15} – 10^{16} cm^{-3} . Taking this circumstance into account, the short-circuit current density in further calculations is set to 26 mA/cm².

Figure 4 shows the “light” I – V characteristic of the CdS/CdTe heterostructure, calculated by formula (10) using (4)–(9) with a carrier lifetime of 10^{-9} s at various resistivities of the absorbing p -CdTe layer.

The barrier height on the semiconductor side in equilibrium $\phi_0 = qV_{bi}$ required for calculations was found as the difference of the energies E_1 and $\Delta\mu$ shown in Fig. 1. The energy E_1 is equal to the CdTe band gap minus two quantities, i.e., the conduction band offset ΔE_c at the CdS–CdTe interface and the distance from the Fermi level to the CdS conduction band bottom $\Delta\mu_{Cds} = kT\ln(N_c/n)$ which, at $n = 10^{16}$ –

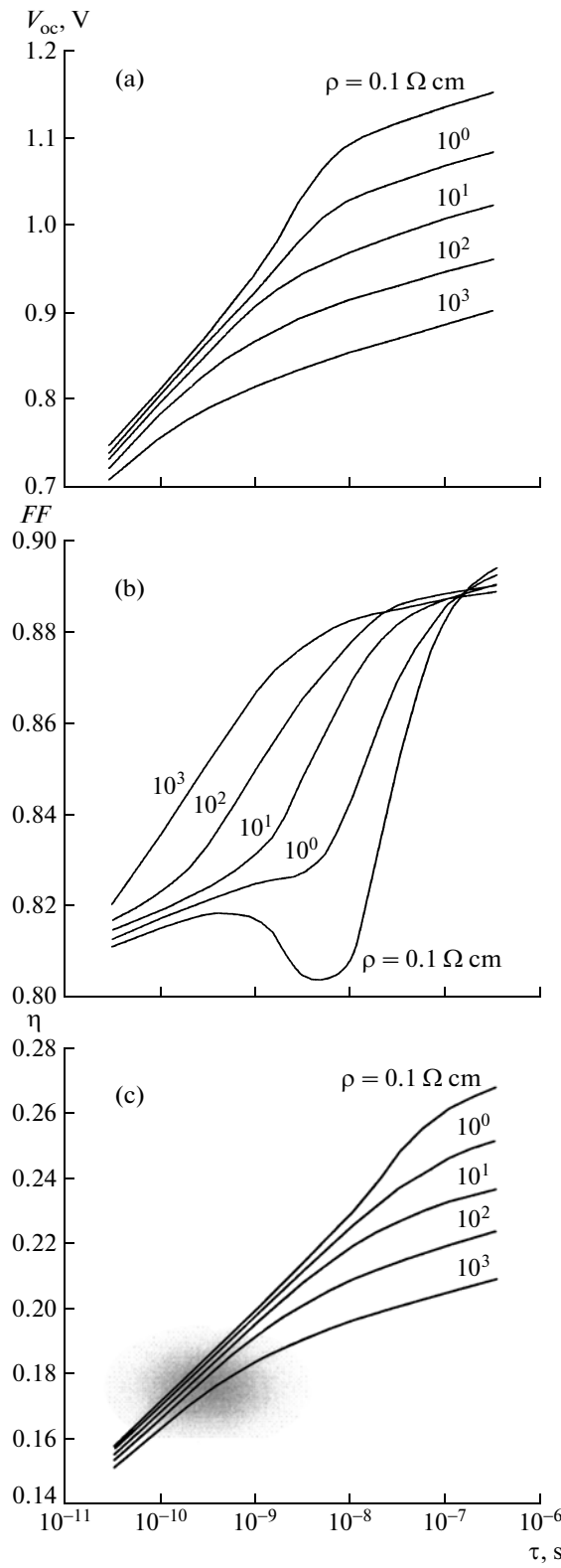


Fig. 5. Dependences of the (a) open-circuit voltage V_{oc} , (b) fill factor FF , and (c) efficiency η of the CdS/CdTe heterostructure on the carrier lifetime τ , calculated for the current found by formula (10) taking into account (4)–(9), at various CdTe layer resistivities ρ (indicated near curves, $\Omega \text{ cm}$). The shaded area corresponds to the results achieved for the best samples of thin-film CdS/CdTe solar cells.

10^{17} cm^{-3} and 300 K yields $\Delta\mu_{\text{CdS}} = 0.08\text{--}0.14 \text{ eV}$ (we disregard the band bending in CdS).

The quantity $\Delta\mu$, i.e., the energy distance from the Fermi level to the top of the valence band in the neutral region of the CdTe layer, is controlled by its resistivity ρ , and ΔE_c is the difference between CdS and CdTe electron affinities χ_{CdS} and χ_{CdTe} . The published data on χ_{CdS} and χ_{CdTe} are rather contradictory; however, the values of χ_{CdS} are more often given within 4.2–4.5 eV [22, 23] and the range of χ_{CdTe} was recently narrowed to 4.2–4.3 eV [14, 24]. Taking the average values of χ_{CdS} and χ_{CdTe} , we find the CdS electron affinity to be higher than that of CdTe by 0.1 eV ($\Delta E_c = 0.1 \text{ eV}$) and $\Delta E_c + \Delta\mu_{\text{CdS}} \approx 0.2 \text{ eV}$. Hence, the barrier height $\phi_0 = qV_{bi} = E_{g\text{CdTe}} - (\Delta E_c + \Delta\mu_{\text{CdS}} + \Delta\mu)$ on the semiconductor side, required for calculations, can be taken as 1.23 eV. We note that the deviation of $\pm 0.1 \text{ eV}$ from the found value of ϕ_0 (certainly, ϕ_0 cannot be lower than the open-circuit voltage) does not lead to appreciable changes in the results of calculation of the open-circuit voltage and fill factor given below. We also note that the voltage drop at the bulk region of the CdTe layer was disregarded in the calculation, since it is negligible at $\rho \leq 10^3 \Omega \text{ cm} (< 0.01 \text{ V})$ [16].

Let us analyze the dependence of the open-circuit voltage, fill factor, and efficiency of the CdS/CdTe solar cell on the carrier lifetime and resistivity of the CdTe absorbing layer. Figure 5a shows the dependences of the open-circuit voltage V_{oc} of the CdS/CdTe heterostructure on the carrier lifetime τ calculated at various resistivities of the CdTe layer.

In the calculation, the range of variation in the carrier lifetime τ is bounded from below by $3 \times 10^{-10} \text{ s}$, since the photocurrent diffusion component is too small at smaller τ ; moreover, the recombination loss in the SCR will become noticeable, if the uncompensated acceptor concentration is below 10^{16} cm^{-3} [11]. The upper limit of ρ ($10^3 \Omega \text{ cm}$) was chosen from the above considerations; the lower limit ($0.1 \Omega \text{ cm}$) corresponds to a rather high hole concentration $p = 10^{18} \text{ cm}^{-3}$ (at the hole mobility $\mu = 60 \text{ cm}^2/(\text{V s})$).

We can see in Fig. 5a that the open-circuit voltage V_{oc} significantly increases as ρ increases and τ decreases. At lifetimes of $10^{-10}\text{--}10^{-9} \text{ s}$, the values $V_{oc} = 0.75\text{--}0.85 \text{ V}$ are far from the maximum possible value ($\sim 1.1 \text{ V}$) to which the curve tends at $\rho = 0.1 \Omega \text{ cm}$ and 10^{-8} s . In the common case when $\tau = 10^{-9} \text{ s}$, the open-circuit voltage V_{oc} increases from 0.8 to 0.9 V as the CdTe resistivity decreases from 10^3 to $0.1 \Omega \text{ cm}$. The sharper increase in V_{oc} at $\rho = 0.1 \Omega \text{ cm}$ in comparison with large ρ is explained by the fact $\Delta\mu$ increasing with ρ , while the barrier for electrons lowers during their drift from CdS to CdTe. As a result, the above-barrier current J_n , i.e., the second term in (10), increases and eventually becomes dominant. The results obtained allow the important conclusion: the existence of the recombination current causes a

decrease in the open-circuit voltage in the CdS/CdTe heterostructure.

Figure 5b shows the dependence of the fill factor $FF = P_{\max}/(J_{sc}V_{oc})$ on the CdS/CdTe structure parameters in the same variation range of the CdTe layer resistivity and the carrier lifetime as in the preceding figure (P_{\max} is the maximum power found from the “light” $I-V$ characteristic as the JV product). We can see that the fill factor FF increases, depending on the material resistivity, as the carrier lifetime increases from 0.8–0.82 to ~ 0.9 , i.e., rather weakly. The non-monotonic variation in FF as a function of τ at $\rho = 0.1 \Omega \text{ cm}$ is explained by the $J-V$ characteristic features shown in Fig. 3 at $\tau_n = 10^{-8} \text{ s}$.

Finally, Fig. 5c shows the dependences of the efficiency $\eta = P_{\max}/P_{\text{inc}}$ of the CdS/CdTe heterostructure on the carrier lifetime at various resistivities of the CdTe layer, where P_{inc} is the power density of AM1.5 solar radiation, corresponding to the entire spectral region, equal to 96.3 mV/cm^2 [25]. We can see that η appreciably increases from 15–16 to 21–27% as the carrier lifetime and resistivity of the CdTe layer increase within the indicated limits. At the carrier lifetime of 10^{-10} – 10^{-9} s , the efficiency is ~ 17 – 18.5% , and a decrease in the CdTe layer resistivity allows an increase in η only by 0.5–1.5% (the shaded area in the figure). As τ increases by an order of magnitude, η increases by $\sim 1\%$ at $\rho = 10^3 \Omega \text{ cm}$ and by 2.5–3% at $\rho = 0.1 \Omega \text{ cm}$ (here, the increase in the short-circuit current density by $\sim 1 \text{ mA/cm}^2$ is disregarded). Thus, if we suppose that $\tau = 10^{-10}$ – 10^{-9} s in the common case, the calculation results appeared to be very close to the efficiency of the best thin-film CdS/CdTe solar cells (16–17%). We recall that the losses for reflection and absorption by the CdS layer were disregarded in the calculation.

7. CONCLUSIONS

The effect of the resistivity ρ and carrier lifetime τ in the CdS/CdTe heterostructure on the open-circuit voltage V_{oc} , fill factor FF , and efficiency η of the solar cell was studied. According to the results obtained, for $\tau = 10^{-10}$ – 10^{-9} s at $\rho = 10^{-1}$ – $10^3 \Omega \text{ cm}$, the solar cell efficiency is within 17–19%, which corresponds to the efficiency of the best thin-film CdS/CdTe solar cells with an absorbing CdTe layer 5 μm thick. It follows from the results obtained that V_{oc} , FF , and η can be substantially increased by improving layers, thus increasing the carrier lifetime τ . For example, as τ increases to 10^{-8} s , η at $\rho = 0.1$ – $10^3 \Omega \text{ cm}$ increases to 20–23%. The efficiency η can be further advanced toward the theoretical limit if τ is increased to 10^{-7} – 10^{-6} s (25–27% provided that $\rho = 0.1$ – $1 \Omega \text{ cm}$). The efficiency η can be increased to 28–30% only at $\tau \geq$

10^{-6} s and an increase in the absorbing layer thickness from 5 to 10–20 μm and even larger. In this case, the short-circuit current density increases to the maximum possible value of 28–29 mA/cm^2 [11].

ACKNOWLEDGMENTS

The authors are grateful to X. Mathew (Energy Research Center-UMAM, Morelos, Mexico) for the thin-film structures put at their disposal and V.M. Sklyarchuk for his assistance in the performance of the experiments.

This study was supported by the State Foundation for Basic Research of Ukraine, contract F14/259-2007.

REFERENCES

1. T. Surek, *J. Cryst. Growth* **275**, 292 (2005).
2. A. Goetzberger, C. Hebling, and H.-W. Schock, *Mater. Sci. Eng. R* **40**, 1 (2003).
3. N. Romeo, A. Bosio, V. Camevari, and A. Podesta, *Sol. Energy* **77**, 795 (2004).
4. J. Britt and C. Ferekides, *Appl. Phys. Lett.* **62**, 2851 (1993).
5. T. Aramoto, S. Kumazawa, H. Higuchi, T. Arita, S. Shibutani, T. Nishio, J. Nakajima, M. Tsuji, A. Hanafusa, T. Hibino, K. Omura, H. Ohyama, and M. Murozono, *Jpn. J. Appl. Phys.* **36**, 6304 (1997).
6. P. V. Meyers and S. P. Albright, *Progr. Photovolt.: Res. Appl.* **8**, 161 (2000).
7. X. Wu, J. C. Keane, R. G. Dhere, C. DeHart, D. S. Albin, A. Duda, T. A. Gessert, S. Asher, D. H. Levi, and P. Sheldon, in *Proc. of the 17th Eur. Photovoltaic Solar Energy Conf.* (Munich, 2001), p. 995.
8. A. Hanafusa, T. Aramoto, and M. Tsuji, *Sol. Energy Mater. Solar Cells* **67**, 21 (2001).
9. D. Bonnet, in *Practical Handbook of Photovoltaic: Fundamentals and Applications*, Ed. by T. Makkvert and L. Castaner (Elsevier, 2003).
10. S. Sze, *Physics of Semiconductor Devices*, 2nd ed. (Wiley, New York, 1981).
11. L. A. Kosyachenko, E. V. Grushko, and A. L. Savchuk, *Semicond. Sci. Technol.* **23**, 025011 (2008).
12. C. Sah, R. Noyce, and W. Shokley, *Proc. IRE* **45**, 1228 (1957).
13. L. A. Kosyachenko, I. M. Rarenko, Z. I. Zakharuk, V. M. Sklyarchuk, E. F. Sklyarchuk, I. V. Solonchuk, I. S. Kabanova, and E. L. Maslyanchuk, *Fiz. Tekh. Poluprovodn.* **37**, 238 (2003) [*Semiconductors* **37**, 227 (2003)].
14. D. Bonnet, in *Clean Electricity from Photovoltaic*, Ed. by M. D. Atcher and R. Hill (Imperial College, 2001), p. 245.
15. J. Fritzsche, D. Kraft, A. Thissen, Th. Mayer, A. Klein, and W. Jaegermann, *Mater. Res. Soc. Symp. Proc.* **668**, 601 (2001).

16. U. V. Desnica, I. D. Desnica-Frankovic, R. Magerle, A. Burchars, and M. Deicher, *J. Cryst. Growth* **197**, 612 (1999).
17. X. Mathew, L. A. Kosyachenko, V. V. Moyushchuk, and O. F. Sklyarchuk, *J. Mater. Sci. Mater. Electron.* **18**, 1021 (2007).
18. L. A. Kosyachenko, O. L. Maslyanchuk, V. V. Motuschchuk, and V. M. Slkyarchuk, *Sol. Energy Mater. Solar Cells* **82**, 65 (2004).
19. L. A. Kosyachenko, V. M. Slkyarchuk, O. F. Slkyarchuk, and V. A. Gnatyuk, *Semicond. Sci. Technol.* **22**, 911 (2007).
20. S. H. Demtsu and J. R. Sites, *Proc. IEEE Photovolt. Specialistsn Conf.* **31**, 347 (2005).
21. J. R. Sites and J. Pan, *Thin. Sol. Films* **515**, 6099 (2007).
22. M. Bujatti, *J. Phys. D: Appl. Phys.* **1**, 581 (1868).
23. K. W. Mitchell, *Evaluation of the CdS/CdTe Heterojunction Solar Cell* (Academic, New York, 1979).
24. T. Takebe, J. Saraie, and T. Tanaka, *Phys. Stat. Solidi A* **47**, 123 (2006).
25. “Reference solar spectral irradiance at the ground at different receiving conditions,” Standard of International Organization for Standardization ISO 9845–1:1992.

Translated by A. Kazantsev